AFOSR TN-59-184
ASTIA AD-211 324

THE UNIVERSITY OF MICHIGAN

COLLEGE OF ENGINEERING

Department of Chemical and Metallurgical Engineering

WHISKER GROWTH ON VANADIUM PENTOXIDE SURFACES

V. J. Lee
G. Parravano

UMRI Project 2832

under contract with:

AIR FORCE OFFICE OF SCIENTIFIC RESEARCH
AIR RESEARCH AND DEVELOPMENT COMMAND
CONTRACT NO. AF 49(638)-493
PROJECT NO. 9762, TASK NO. 37621
WASHINGTON, D. C.

administered by:

THE UNIVERSITY OF MICHIGAN RESEARCH INSTITUTE ANN ARBOR

March 1959

ACKNOWLEDGEMENT

We wish to thank Drs. C. W. Allen and K. Igaki for taking the measurements on growth rate.

ABSTRACT

The growth of whiskers has been observed on single crystals and polycrystalline samples of vanadium pentoxide. Detailed data on the growth rate are presented for temperatures 546 to 650°C in air, steam and vacuum, for closed and open atmospheres. From the kinetic expressions a growth mechanism has been derived. The mechanism involves gas phase condensation and surface diffusion on the whisker top together with bulk diffusion within the whisker. The interplay of different factors in determining the type of growth is discussed. In open systems, whiskers were found to grow by diffusion from the base, while evaporation was predominant at the top. Whiskers, which upon growing on the surface of a vanadium pentoxide microsphere at uniform cross section, meet a neighboring sphere, grow suddenly in diameter. It is suggested that whisker formation represents the first stage of sintering of vanadium pentoxide particles.

INTRODUCTION

Filamentary growth on solid surfaces has been investigated for mono- and multicomponent solids, the latter group including mainly daltonide compounds[1]. The majority of these studies have been concerned with a growth mechanism involving a diffusional process along the whisker surface and gas phase mass transfer under the influence of a high supersaturation radio. The question arises, however, as to what extent a similar mechanism is responsible for the filamentary growth on other types of substances. In the case of berthollide compounds, for instance, their non-stoichiometric nature may induce growth patterns differing from those recorded for metals and essentially stoichiometric metallic salts.

We have observed filamentary growth on various non-stoichiometric metal oxides (V_2O_5, ZnO, TiO_2) and we have studied growth characteristics on V_2O_5 in more detail. The results of these observations are reported in this communication, together with data on the rate of growth of V_2O_5 whiskers under different experimental conditions. As it will be shown, gas phase mass transfer is only partially responsible for whisker growth on V_2O_5, a large contribution to the total growth being due to diffusional transport within the solid phase.

EXPERIMENTAL

Whisker growth on V_2O_5 was followed on single crystals and polycrystalline samples. Large crystals of V_2O_5 (Baker, analyzed) were produced by the Bridgman method in a fused quartz tube. Crystals of about 2 cm. long, 1 cm. wide and a few mm. thick were obtained by cleaving the large specimens. The orientation of the smaller crystals was determined from back reflection x-ray patterns and from etch pit observations[2]. The crystals were fastened to a chunk of polycrystalline V_2O_5 by means of a paste of V_2O_5 in distilled water. The polycrystalline aggregate of V_2O_5 served as excess oxide in the system and as a support for locating the crystal to be observed. The assembly was snugly fitted in a fused quartz tube (10 mm. diameter), closed at one end and with a portion of the wall previously flattened to permit microscopic examination inside the tube. The tube with the V_2O_5 specimen was evacuated at 300°C for one hour and afterward sealed under vacuum or the desired gas atmosphere. The entire closed system was fitted in a stainless steel block housed in a muffle furnace, kept at constant temperature (± 5°C) for different amounts of time. At the end of a series of runs x-ray patterns failed to show any differences between the base crystal and the same at the beginning of the investigation. When using water vapor as surrounding atmosphere, dissolved air was removed by repeated freezing and melting.

Whisker growth was also followed on polycrystalline

spheres of V_2O_5 obtained from molten V_2O_5 by dropping it through a blast of purified air. The spheres (diameter $\sim$ 0.7 mm.) were inserted in a small Pt boat, located inside a well type muffle, kept at constant temperature ($\pm 2°C$). A slow stream of purified air was passed on the spheres during a run (open system).

Observations of whiskers growing on the single crystal base were made by removing the quartz tubing with the sealed sample from the furnace and cooling it at room temperature. A Bausch and Lomb research metallograph was employed and measurements of whisker length were accomplished by means of a Feiler stage. For the system employing V_2O_5 microspheres, data were taken by means of a Gaertner creep test microscope, fitted with a bifilar eyepiece. The microscope was arranged directly above the Pt boat so that measurements on whisker length could be taken at the temperature of the run.

RESULTS

The general morphological aspects of the whiskers studied can be observed in Figs. 1 to 3. Fig. 1 shows a large number of whiskers growing out of joined polycrystalline microspheres in the open air system. Fig. 2 shows some whiskers grown on a single crystal. In this instance it was observed that the shape of the whiskers was affected by the atmosphere; air grown whiskers had a tendency to be cone shaped (Fig. 2a), while vacuum or steam grown ones attained much longer lengths (up to 1 mm.) with apparently uniform cross section (Fig. 2b). Visual observation established that only air grown whiskers were dependent on the orientation of the V_2O_5 substrate crystal. In this case growth occurred preferentially in a direction parallel to the c-axis. This is consistent with the known fact that V_2O_5 crystals grow much faster along this axis as compared to the other two[2].

In addition to whisker growth, the formation of long narrow crystals was observed in most runs (Fig. 3). A large concentration of these fine crystals was observed on vacuum or steam treated samples.

Typical growth rate curves for single crystals and polycrystalline samples are recorded in Figs. 4, 5, 6, and 7 for temperatures up to 650°C, in air, vacuum or steam atmosphere. In Figs. 6 and 7 data are also presented on the width of the whiskers. Sometimes the length of a whisker decreased with increasing time and some whiskers disappeared suddenly and completely from the eyefield.

DISCUSSION

It is instructive to investigate briefly the thermodynamic conditions under which whiskers are present and grow before attempting to interpret the mechanism of their growth. Let p_o and p be the vapor pressure in equilibrium on a flat surface and on the top of a whisker of V_2O_5 respectively; the value of the ratio p/p_o can be computed by means of the Thomson relationship:

$$\ln \frac{p}{p_o} = \frac{2V}{RT} \frac{\gamma}{s}$$

where V is the molar volume, s the radius of curvature of the tip of the whisker and γ the surface energy. Taking $V = 54.3$ cc, $s = 3\mu$, $\gamma \approx 750$ erg/cm^2, it is found p/p_o 10^{11} at 600°C. This, of course, indicates that whiskers are highly unstable with respect to the surface on which they grow. The mechanism of their stabilization must be sought in the presence of dislocations or other types of line or plane imperfections, which, although unstable, cannot be removed sufficiently fast from the crystal. These defects provide a very effective energy sink along the whisker structure and at the whisker top. In fact, using the order of magnitude of our previous computation, the tip of the whisker will have a net positive difference of chemical affinity over that of the flat surface, equal to $-RT \ln 1/p_o \cong$ $\cong +41$ kcal/mole.

The presence of a line defect has the result of decreasing this quantity to a value lower than that competing to the flat surface.

The resulting picture of the surface is a very heterogeneous one, and the presence of filamentary growth on solid surfaces can be taken as a striking demonstration of their energetic heterogeneity.

Furthermore, the thermodynamic conditions existing around a whisker must have an effect on the chemical composition of the whisker top because of the non-stoichiometric nature of V_2O_5. In the present case, it is safe to assume that the whisker top possesses a larger number of point defects relative to the underlying bulk phase. The possibility cannot be excluded that the defect density in the whisker is so large that defect clustering occurs and a new phase (a lower oxide?) is nucleated. The high concentration of point defects has a profound effect in several ways on the dislocations, their interactions and movements within the whiskers.

Essentially, whisker growth can occur by two mechanisms: gas phase condensation on and around the whisker top and diffusion within and/or on the whisker. The first mechanism is a distillation process controlled by a vapor pressure difference, while the second involves a gradient of concentration. The former mechanism has been repeatedly invoked to explain the growth of metallic whiskers[1], while the latter one has been discussed as a theoretical possibility[3].

For both processes one must assume the presence of at least one dislocation within the whisker. The dislocation, upon meeting the whisker surface or through its core, provides a sink for gas phase molecules and lattice defects, and, as a consequence, may be held responsible for the observed growth.

Growth by Gas Phase Condensation

We shall analyze first the mechanism of growth by gas phase condensation.

Let:

σ = surface density ($m \times \ell^{-2}$)

$= p\left(\frac{M}{2\pi RT}\right)^{1/2}$ = mass flux of molecules striking at the whisker surface per unit time ($m \times \ell^{-2} \times t^{-1}$)

v = absolute linear velocity of climb of molecules toward the whisker top ($\ell \times t^{-1}$)

$u = \frac{d\ell}{dt}$ = average linear rate of whisker growth during the time interval from 0 to t ($\ell \times t^{-1}$).

$\Delta v = (v - \frac{d\ell}{dt})$ = molecular linear velocity along the whisker surface relative to the rate of growth of the top ($\ell \times t^{-1}$).

Taking a mass balance across the whisker, one gets:

$$\pi r^2 \varsigma \frac{d\ell}{dt} = \pi r^2 \varphi + 2\pi r \Delta v \sigma \qquad (1)$$

where ς and r are the whisker density and radius, respectively. From (1):

$$\frac{d\ell}{dt} = \frac{\varphi}{\varsigma} + \frac{2\sigma}{r\varsigma} \Delta v \qquad (2)$$

In equation (2), $\sigma = \sigma(t)$. Therefore, in the subsequent discussion we shall distinguish two stages: 1. An initial stage corresponding to an unsteady state during which the rate of growth increases with time. We assume that this period of growth is defined by $\ell \simeq \ell_s$, where $\ell_s = vt_s$ and t_s is the average lifetime of an adsorbed molecule before re-evaporation under conditions of adsorption equilibrium; 2. A steady state process during which the rate of growth is constant at the maximum value. For this stage $\ell \gg \ell_s$. We shall deduce first the form of equation (2) for the initial stage. Let us consider a rectangular area, $\ell \times z$, on the whisker surface, and $d\sigma$ = the change in surface density during an interval dt. A mass balance across the area ℓz during the time dt gives:

$$\frac{d\sigma}{dt} + \frac{\Delta v}{\ell}\sigma = \varphi, \quad \text{or:}$$

$$\sigma = \frac{\varphi \ell}{\Delta v}\left[1 - \exp\left\{-\frac{\Delta v t}{\ell}\right\}\right] \qquad (3)$$

and by substitution into (2)

$$\frac{d\ell}{dt} = \frac{\varphi}{\rho}\left[1 + \frac{2\ell}{r}\left(1 - \exp\left\{-\frac{\Delta v t}{\ell}\right\}\right)\right] \qquad (4)$$

Equation (4) describes the rate of growth during the initial period and shows that growth is a complex, but nearly exponential, function of time.

Let us now consider stage 2 of growth, and let $\ell = ut$, where $u = \left(\frac{d\ell}{dt}\right)_{average}$ during the time t, and

$$\sigma = \frac{\varphi \ell}{\Delta v}\left[1 - \exp\left\{-\frac{\Delta v}{u}\right\}\right] \tag{5}$$

where σ is now the average surface density over the length $\int_0^t \frac{d\ell}{dt}\,dt$. σ will reach its maximum value for $\ell = \ell_s = vt_s$. We can then set $\ell_s = vt_s = ut$ and:

$$t = \frac{vt_s}{u} \tag{6}$$

Substituting (6) into (5) and the resulting equation into (2) and since $vt_s = \ell_s$

$$\left(\frac{d\ell}{dt}\right)_{max} = \frac{\varphi}{\varsigma}\left[1 + \frac{2\ell_s}{r}\left(1 - \exp\left\{-\frac{\Delta v}{u}\right\}\right)\right] \tag{7}$$

Equation (7) describes the rate of growth of the whisker after the initial period. Since at constant temperature, the right member of equation (7) is constant, growth will, during this stage, follow a linear rate. By putting $\Delta v = \infty$ in equation (7) one obtains:

$$\left(\frac{d\ell}{dt}\right)_{max} = \frac{\varphi}{\varsigma}\left(1 + \frac{2\ell_s}{r}\right) \tag{8}$$

This equation has been previously derived to interpret the growth of metallic whiskers[1c]. It can be seen that equation (8) is correct for $\Delta v = \infty$ only. This, of course, is physically impossible. In practice, however, Δv is large enough and the approximation involved in the use of equation

(8) is quite sufficient to fit the experimental data.

Growth by Gas Phase Condensation and Bulk Diffusion. Closed System.

Let us now consider the general case in which both processes of gas phase condensation and bulk diffusion contribute to the growth of the whisker. Letting D_v = atomic diffusion coefficient, a mass balance across the whisker for an interval of time Δt during which the whisker has grown by $\Delta \ell$ gives:

$$\pi r^2 \Delta \ell \rho = \pi r^2 \varphi \left[1 + \frac{2\ell_s}{r}\left(1 - \exp\left\{-\frac{\Delta v}{u}\right\}\right)\right]\Delta t + \pi r^2 D_v \left(\frac{\Delta C}{\ell}\right)\Delta t \qquad (9)$$

where ΔC = concentration difference (gr/cc) due to point defects or vacancies between whisker top and bulk solid phase (ΔC has a negative value). The first term of the right hand side of equation (9) is obtained from equation (7) and gives the contribution of the gas phase condensation process, while the second term expresses the mass increase of the whisker due to bulk diffusion. This term is easily obtained by taking a mass balance across the whisker under the assumption that growth is due to bulk diffusion only.

Taking limits and rearranging equation (9) one gets:

$$\frac{d\ell}{dt} = a + \frac{b}{\ell} \qquad (10)$$

where:

$$a = \frac{\varphi}{\rho}\left[1 + \frac{2\ell_s}{r}\left(1 - \exp\left\{-\frac{\Delta v}{u}\right\}\right)\right]$$

$$b = \frac{D_v \Delta C}{\rho}$$

Equation (10) represents the growth rate of whiskers by means of gas phase condensation, and bulk diffusion, and shows the interplay of the various parameters in determining the relative contribution of each mechanism to the total growth.

Rearranging equation (10) integrating and assuming $l = 0$ for $t = 0$, one obtains:

$$al + b \ln \frac{b}{al+b} = a^2 t$$

or:

$$l = \frac{b}{a}\left[\exp\left\{\frac{a}{b}(l - at)\right\} - 1\right] \qquad (11)$$

Equation (11) can be expanded into a convergent power series in terms of $\frac{a}{b}(l - at)$, giving:

$$l = (l - at) + \frac{1}{2!}(l-at)^2 + \frac{1}{3!}(l-at)^3 + \cdots$$
$$\cdots + \frac{1}{n!}\left(\frac{a}{b}\right)^{n-1}(l-at)^n + \cdots \qquad (12)$$

The rapidity of convergence of this series is dependent on $\frac{a}{b}(l - at)$; a and b are constant at constant temperature and $(l - at)$ is the net length of whisker contributed by bulk diffusion. With sufficient approximation, one can consider the first two terms only of series (12):

$$l \geq (l - at) + \frac{1}{2!}\frac{a}{b}(l - at)^2 \qquad (13)$$

Since the total whisker length due to the combined mechanisms is longer than the length contributed by gas phase condensation alone, it is possible to rearrange equation (13) and get:

$$at < \ell \leq at + (2bt)^{1/2} \tag{14}$$

In equation (14) the equality sign holds exactly for a = 0 or b = 0, and it is a good approximation for small values of $(\ell - at)$. For a = 0, one gets:

$$\ell = (2bt)^{1/2}$$

which is the parabolic rate of growth. Equation (14) can be rearranged as follows:

$$at^{1/2} < \frac{\ell}{t^{1/2}} \leq at^{1/2} + (2b)^{1/2} \tag{15}$$

According to equation (15) and for an interval of time not too long, a plot of $\ell/t^{1/2}$ vs $t^{1/2}$ should yield a straight line parallel to the line $\ell/t^{1/2} = at^{1/2}$. However, even for infinite time the deviation of the former from a straight line should be less than $(2b)^{1/2}$.

In Figure 8 the experimental data obtained in the closed system (air,vacuum) at 650°C where both processes contribute to growth have been plotted according to equation (15). The

fit is quite satisfactory thus confirming the foregoing analysis and giving supporting evidence for the contribution of gas phase condensation and surface and bulk diffusion to whisker growth on V_2O_5.

At lower temperatures (570°C) the linear rate predominates (Fig. 5) indicating that growth is almost wholly controlled by gas phase and surface processes.

Growth in Open System.

When whiskers are grown in an open system, the thermodynamic conditions for growth through gas phase transport are drastically altered since evaporation from the top may become predominant over condensation. If E = net rate of evaporation ($m \times t^{-1} \times \ell^{-2}$), the rate of growth under these conditions becomes:

$$\frac{d\ell}{dt} = \frac{D_v \Delta C}{\ell} - \frac{E}{\varsigma}$$

or:

$$\frac{d\ell}{dt} = \frac{b}{\ell} - c \qquad (16)$$

where $c = \frac{E}{\varsigma}$.

Rearranging and integrating equation (16), one gets:

$$-\ell = \frac{b}{c}\left[\exp\left\{-\frac{c}{b}(\ell + ct)\right\} - 1\right] \qquad (17)$$

Equation (17) can be expanded into an alternating, convergent series:

$$l = (l+ct) - \frac{1}{2!}\left(\frac{c}{b}\right)(l+ct)^2 + \frac{1}{3}\left(\frac{c}{b}\right)^2(l+ct)^3 + \ldots$$

$$+ \ldots (-1)^{n-1}\left(\frac{c}{b}\right)^{n-1}(l+ct)^n + \ldots$$

Taking as an approximation the first two terms of the right side of the above series, one gets:

$$l \geq (l+ct) - \frac{1}{2}\left(\frac{c}{b}\right)(l+ct)^2$$

and therefore,

$$l \geq (2bt)^{1/2} - ct$$

or, more generally,

$$\left(\frac{2D_v \Delta C}{S}\right)^{1/2} > \frac{l}{t^{1/2}} \geq \left(\frac{2D_v \Delta C}{S}\right)^{1/2} - \frac{E}{S}t^{1/2} \qquad (18)$$

According to equation (18), the data expressing the rate of growth in open systems should fit into a straight line with negative slope when plotted as $l/t^{1/2}$ vs $t^{1/2}$. Our data, obtained in an open system are shown in Fig. 9 to conform to the requirements of equation (18) in a satisfactory manner.

The maximum length of the whiskers, l_m, will be obtained when:

$$\frac{D_v \Delta C}{\rho \ell_m} = \frac{E}{\rho} \quad , \quad \ell_m = \frac{D_v \Delta C}{E}$$

or: $b = c\ell_m$ (19)

Substitution of equation (19) into (16) and integrating, one gets:

$$\left(\frac{\ell}{\ell_m}\right) + \left(\frac{c}{\ell_m}\right) t = -\ell_n \left[1 - \frac{\ell}{\ell_m}\right] \tag{20}$$

Since $\frac{\ell}{\ell_m} < 1$, it is possible to expand equation (20) into a convergent, infinite series:

$$\sum_{n=2}^{n=\infty} \frac{1}{n} \left(\frac{\ell}{\ell_m}\right)^n = \left(\frac{c}{\ell_m}\right) t \tag{21}$$

During the initial stages of growth, when $\ell \ll \ell_m$, the relationship between t and ℓ is nearly quadratic, while it will change over to a higher power as the whisker length increases. If, during growth, diffusion within the whisker is suddenly stopped or blocked, the whisker will disappear quickly; the rate of disappearance being given by $-\frac{E}{\rho}$. If the blocking agent is removed before the whisker has disappeared completely, the whisker will start to grow again according to equation (21). This may explain our experimental observations on some whiskers which seemed to shorten and grow "at will" or disappear completely.

Radial Growth of Whiskers

In the open system, whenever a growing whisker from one microsphere collided with another sphere, purposely set at some distance (~0.1 mm) from the first one, the whisker suddenly grew radially. Kinetic data on this effect are reported in Fig. 7.

Upon collision with the adjacent sphere, the whisker will tend to bend, and as a result different parts of it will be subjected to tensile and compression stresses. There will be also a shear component which can rapidly reach values above the critical shear stress of the V_2O_5 whisker. The shear stress will produce slip and dislocations[4]. Possibly the vacancy concentration is also a function of the stress and as a result a concentration gradient between the bulk of the two microspheres and the whisker surface will be set up. Then the mass flux through the cross section of one of the ends of the whisker is:

$$2 D_v \pi r^2 \Delta C \Big/ \left(\frac{l_f^2}{4} + r^2\right)^{1/2}$$

where l_f = final length of whisker.

Taking a mass balance at one of the whisker's base during a time dt, during which the radius has grown by dr, and since $l_f >> r$, one obtains:

$$(dr/r) = \left\{ (D_v \Delta C) \Big/ \rho l_f \left[(l_f^2/4) + r^2 \right] \right\} dt$$

which, upon integration, gives:

$$\ell\left(\frac{r}{q}\right) = \frac{2 D_v \Delta C}{\rho l_f^2} t$$

or:

$$r = q \exp\left\{ \frac{2 D_v \Delta C}{\rho l_f^2} t \right\} \qquad (22)$$

where q is the integration constant.

Putting $g = \frac{2D_v \Delta C}{S l_f^2}$ and setting $r = r_c$ at the time of contact ($t = t_c$) of the whisker top with the adjacent sphere, we have from equation (22):

$$r_c = q \exp\{g t_c\} \tag{23}$$

From equations (22) and (23), one obtains:

$$r = r_c \exp\{g(t - t_c)\}$$

or:

$$\log D = \log D_c + g(t - t_c) \tag{24}$$

where D is the diameter of the whisker. According to equation (24) a plot of $(t - t_c)$ vs log D should yield a straight line. The experimental data on the radial growth have been plotted according to equation (24) in Fig. 10.

As r increases, a value will be reached where the condition $l_f \gg r$ will no more be valid, and consequently the rate of growth will change. At this stage, the whisker radius will be large, the whisker being transformed in a neck connecting the two microspheres. These will now be sintering together. Under these conditions, the rate of growth of the neck is approximately $D \propto t^4$ (5). We are thus led to suggest that whisker growth provides the initial stage for the sintering of V_2O_5. The overall process is schematically represented in Fig. 11.

BIBLIOGRAPHY

1. a. J. D. Eshelby, Phys. Rev., 91, 755 (1953).

   b. R. M. Fisher, L. S. Darken, K. G. Carroll, Acta Met. 2, 370, (1954).

   c. G. W. Sears, ibid 3, 361, 367, (1955).

   d. W. J. Courtney, J. Chem. Phys. 27, 1349, (1957).

   e. R. V. Coleman, G. W. Sears, Acta Met., 5, 131, (1957).

   f. R. V. Coleman, N. Cabrera, J. Appl. Phys. 28, 1360 (1957).

   g. J. Franks, ibid 6, 103, (1958).

2. A. Bystrom, K. A. Wilhelmi, O. Brotzen, Acta Chem. Scand., 4, 1119 (1950).

3. M. O. Peach, J. Appl. Phys. 23, 1401, (1952).

4. W. R. Hibbard, C. G. Dunn, Acta Met. 4, 306, (1956).

5. V. J. Lee, G. Parravano: Unpublished observations.

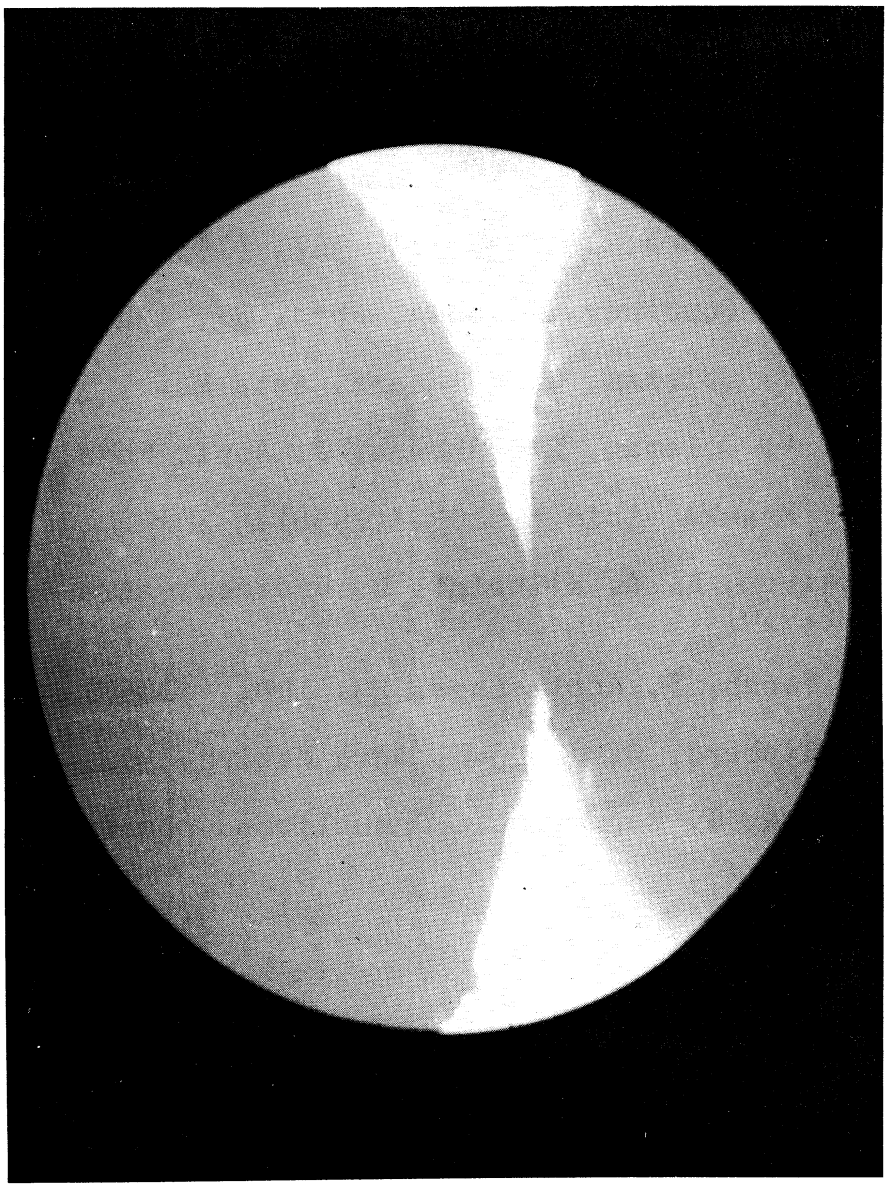

Fig. 1. Whisker growth on polycrystalline spheres of vanadium pentoxide; 580°C, open air system, 10 hours, 96X.

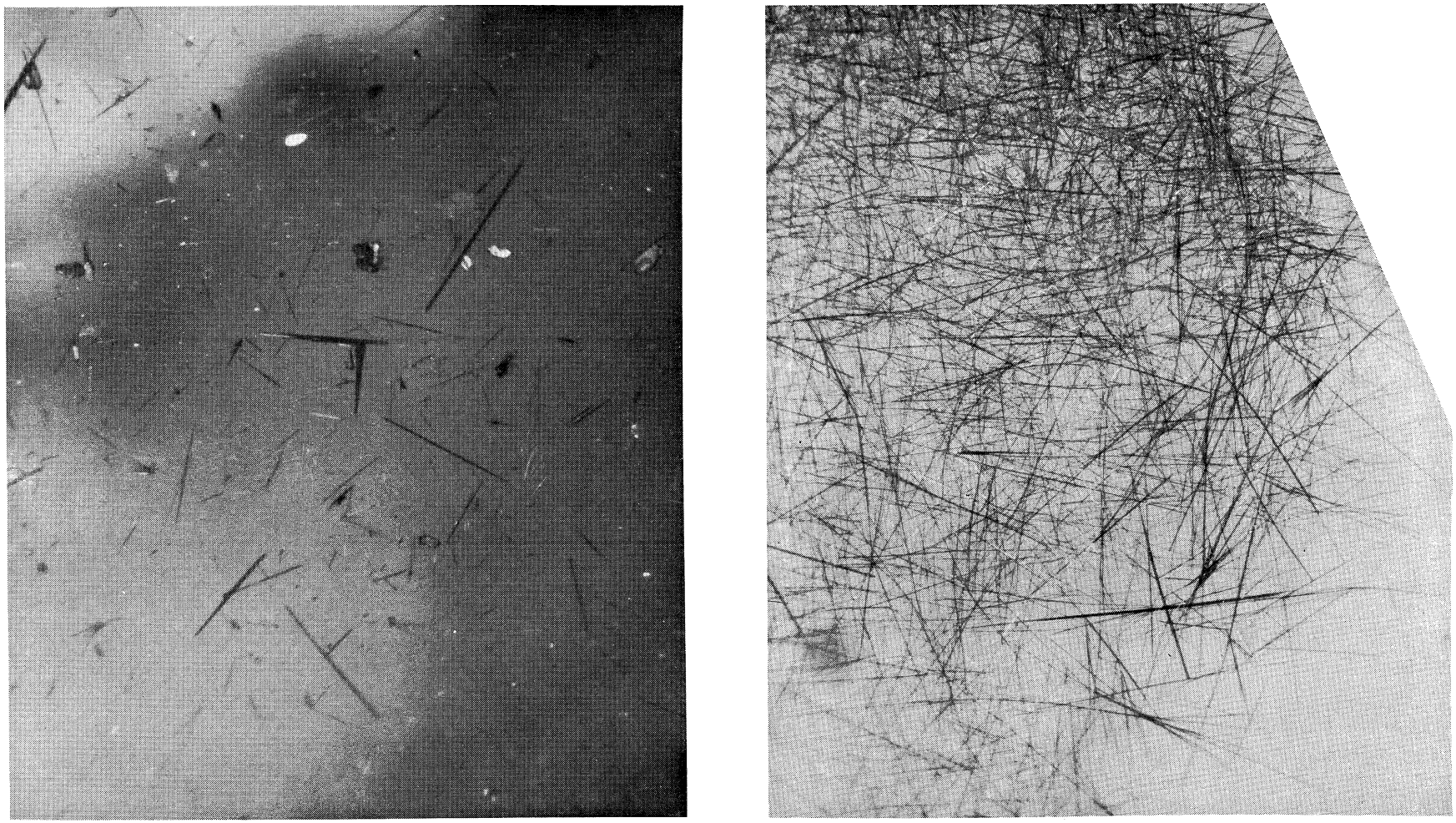

a. Air grown, 8 hours, 100X.

b. Vacuum grown, 6 hours, 69X.

Fig. 2. Vanadium pentoxide whiskers, 650°C, closed system.

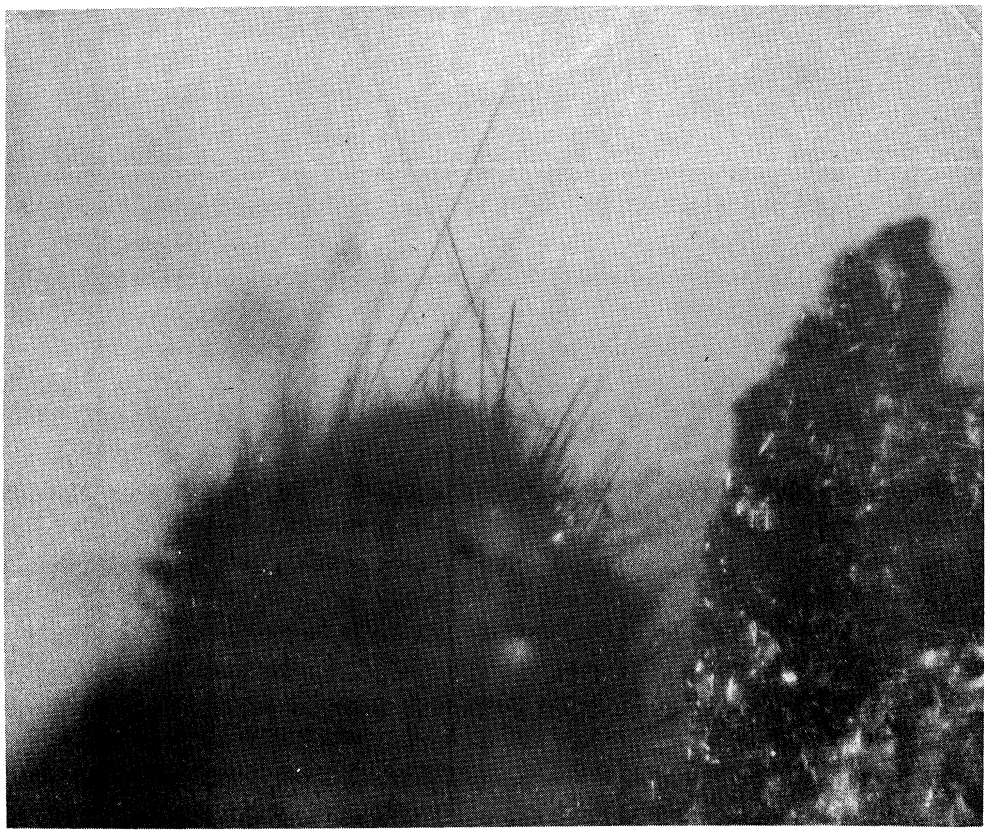

a. Air grown, 8 hours, 100X.

b. Steam grown, 20 min., 100X.

Fig. 3. Vanadium pentoxide ferns, 650°C, closed system.

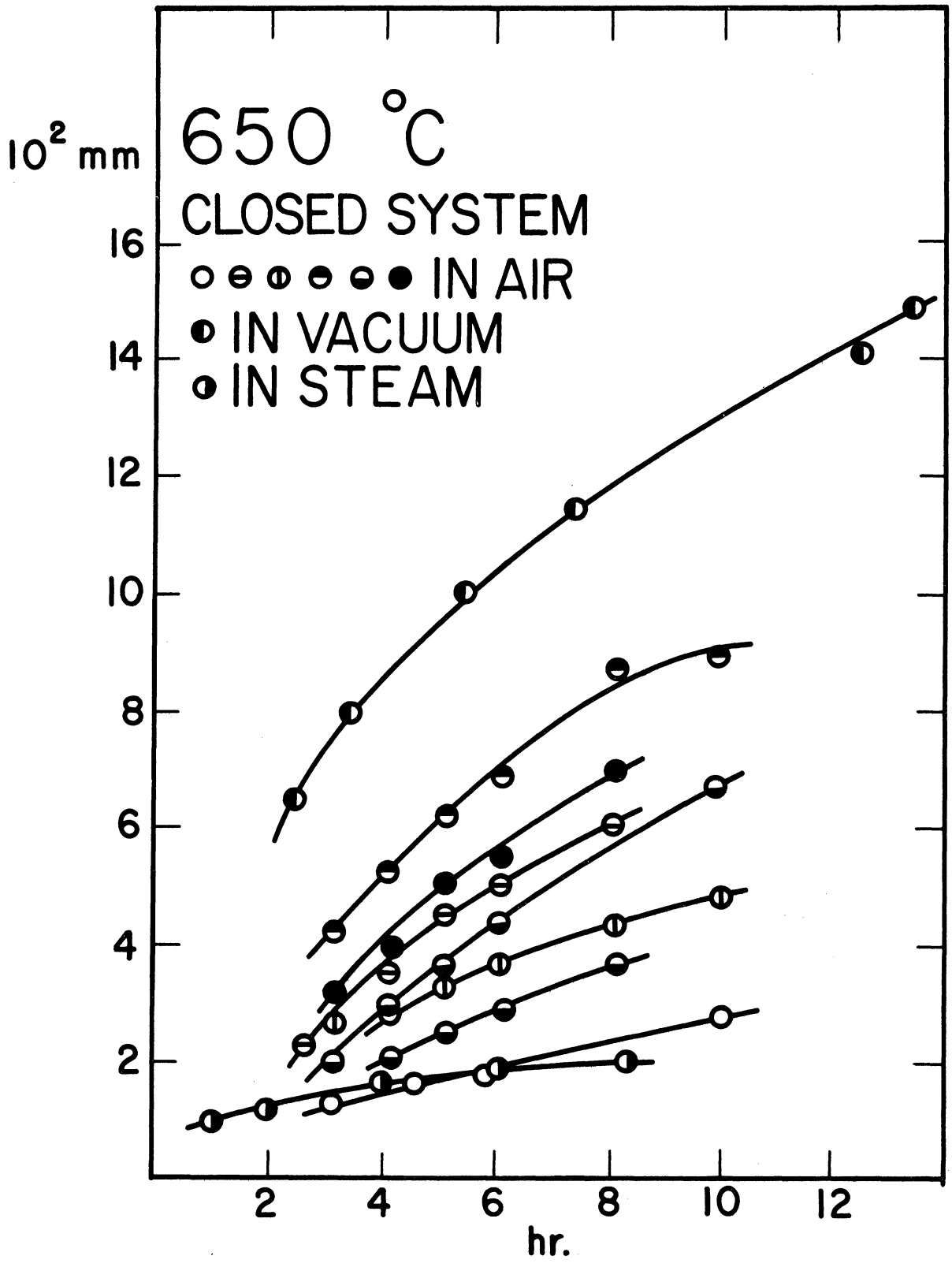

Fig. 4. Growth of individual vanadium pentoxide whiskers.

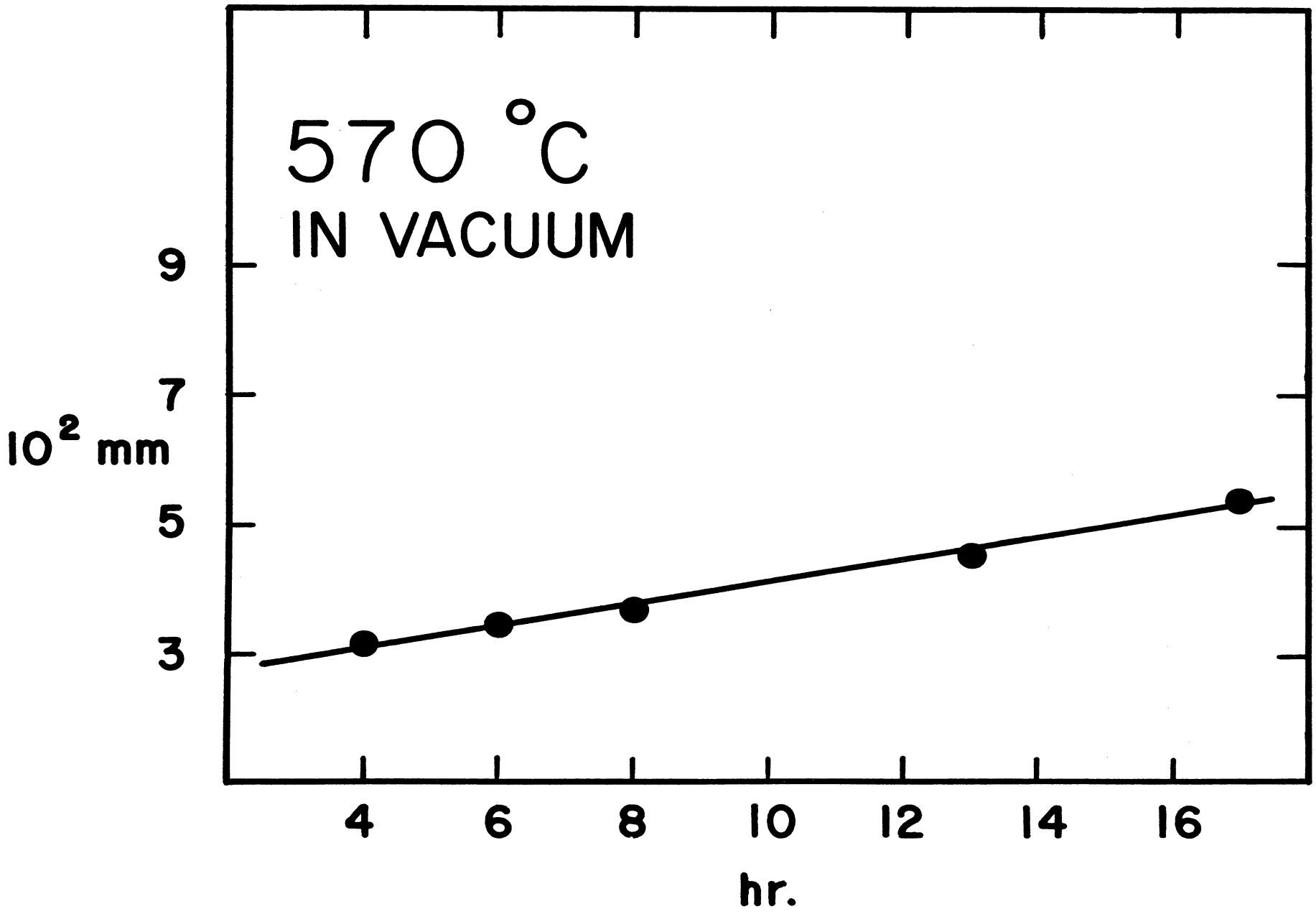

Fig. 5. Growth of vanadium pentoxide ferns.

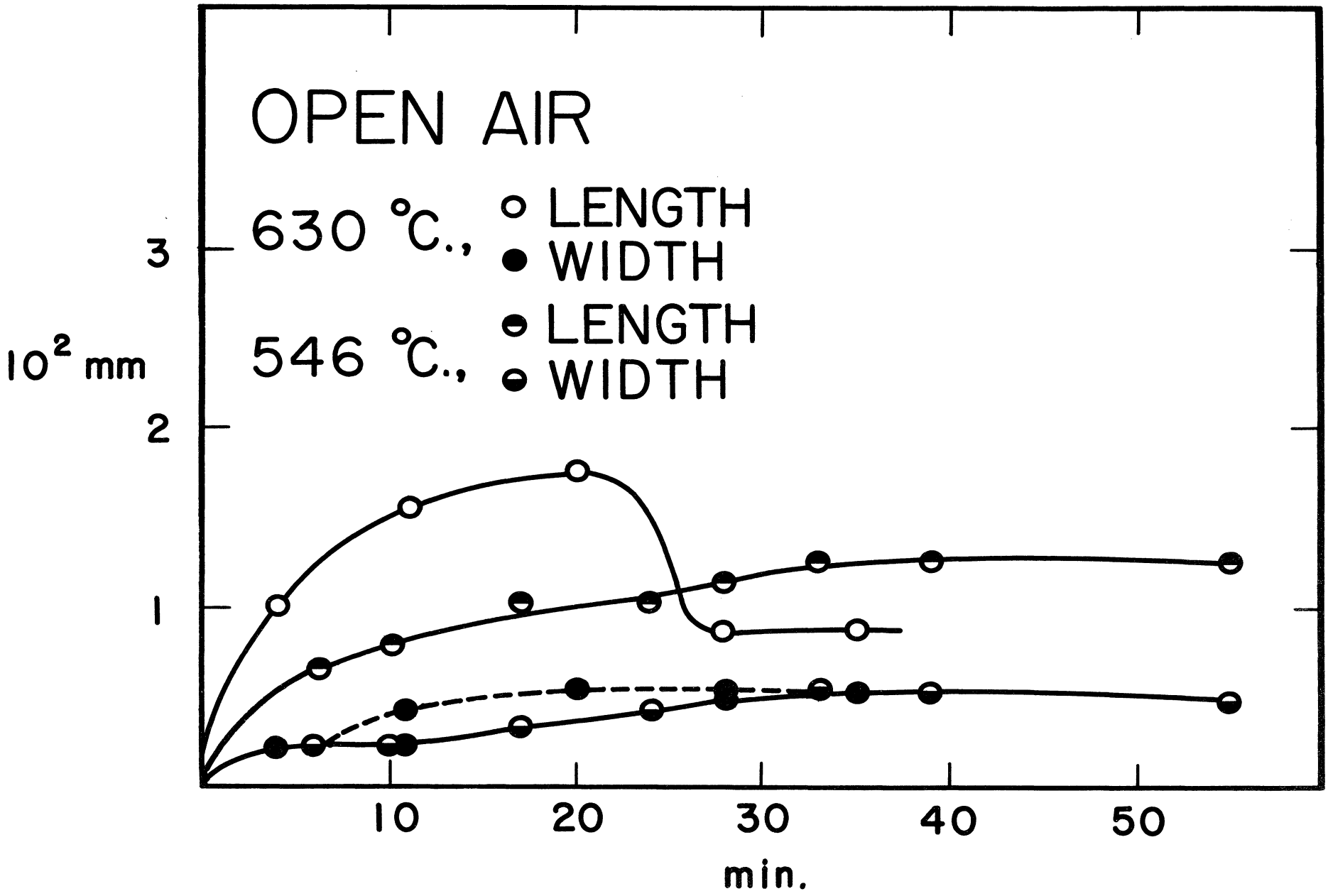

Fig. 6. Growth of individual vanadium pentoxide whiskers.

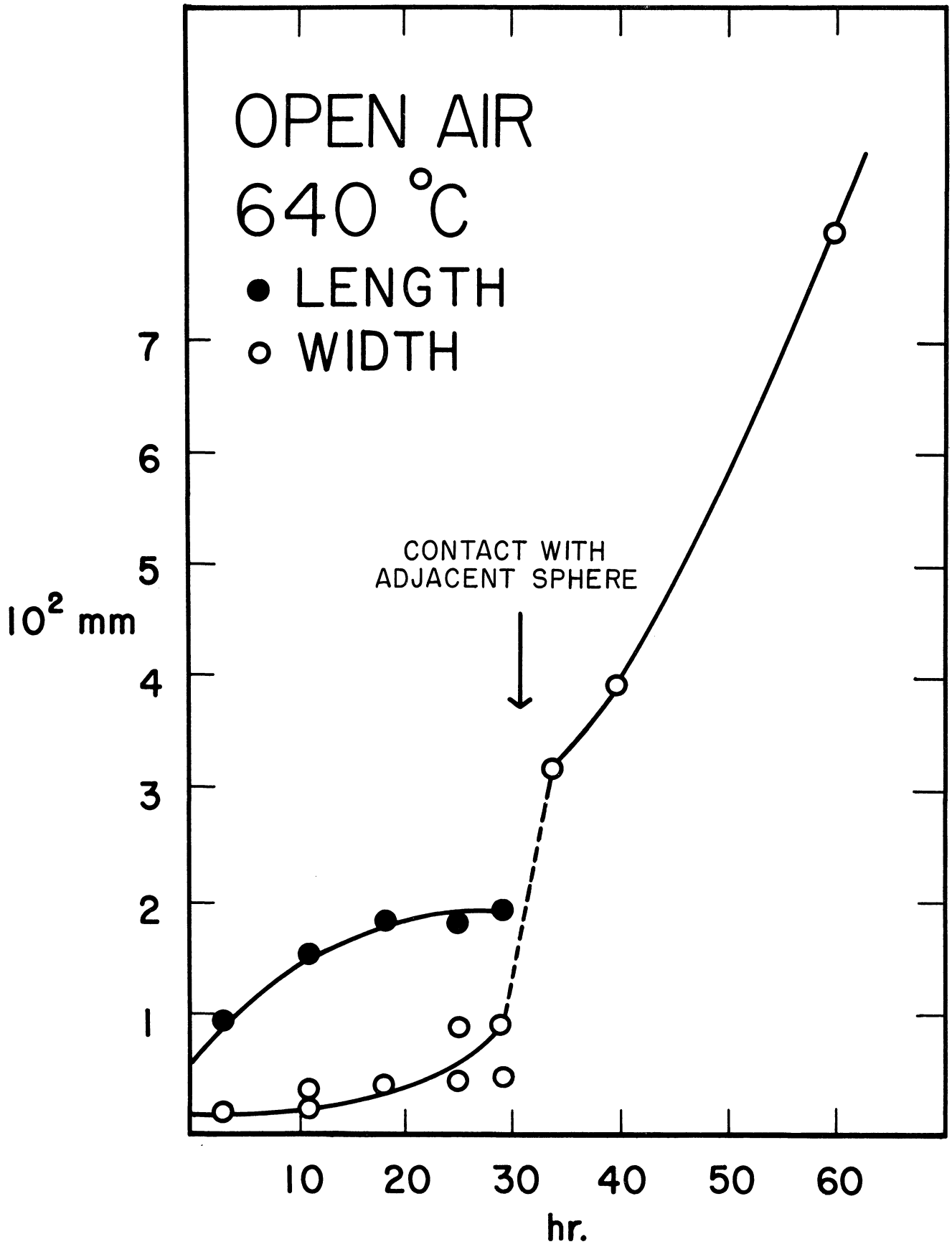

Fig. 7. Growth of individual vanadium pentoxide whiskers.

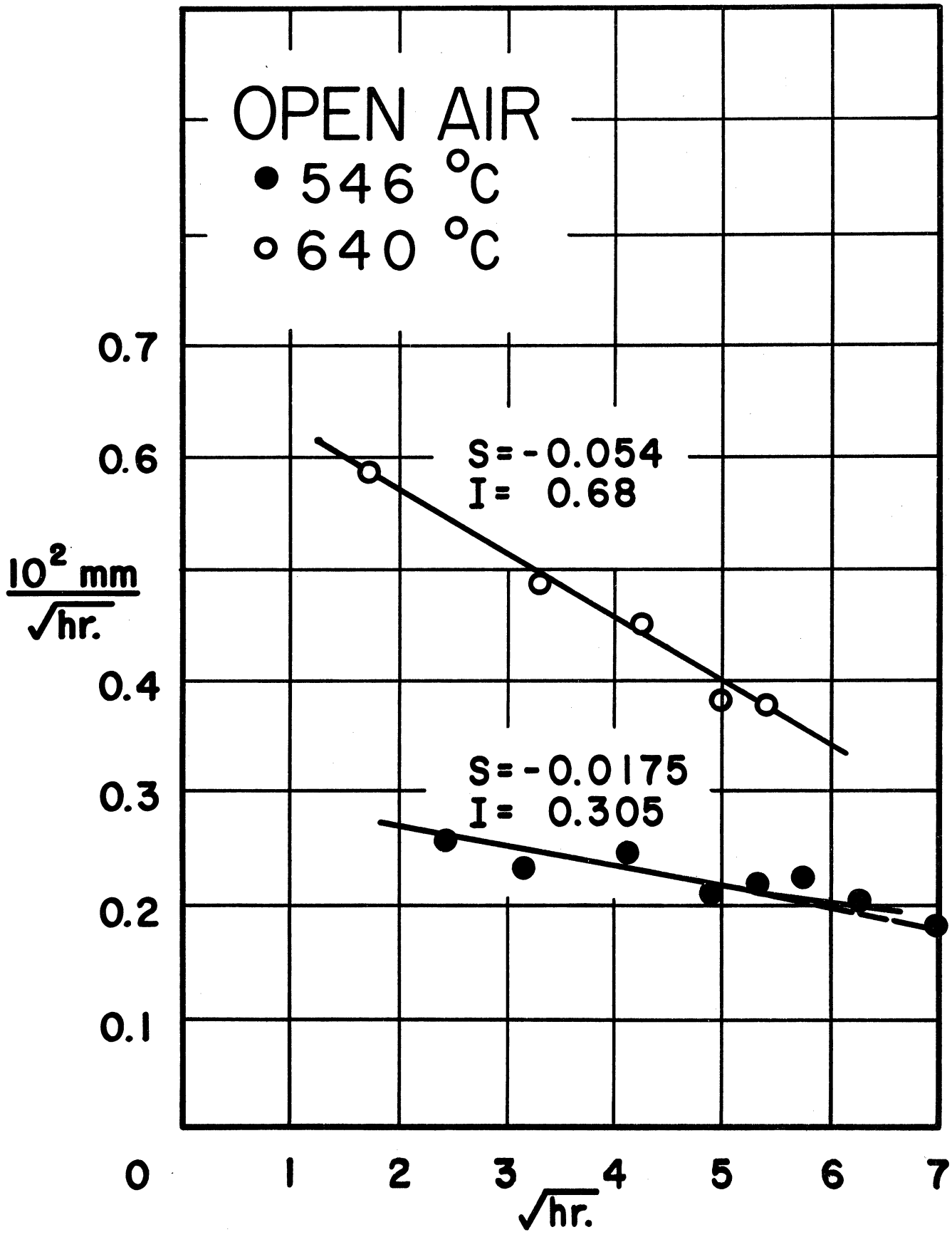

Fig. 9. Growth of individual whiskers of vanadium pentoxide for open system, plotted according to equation (18).

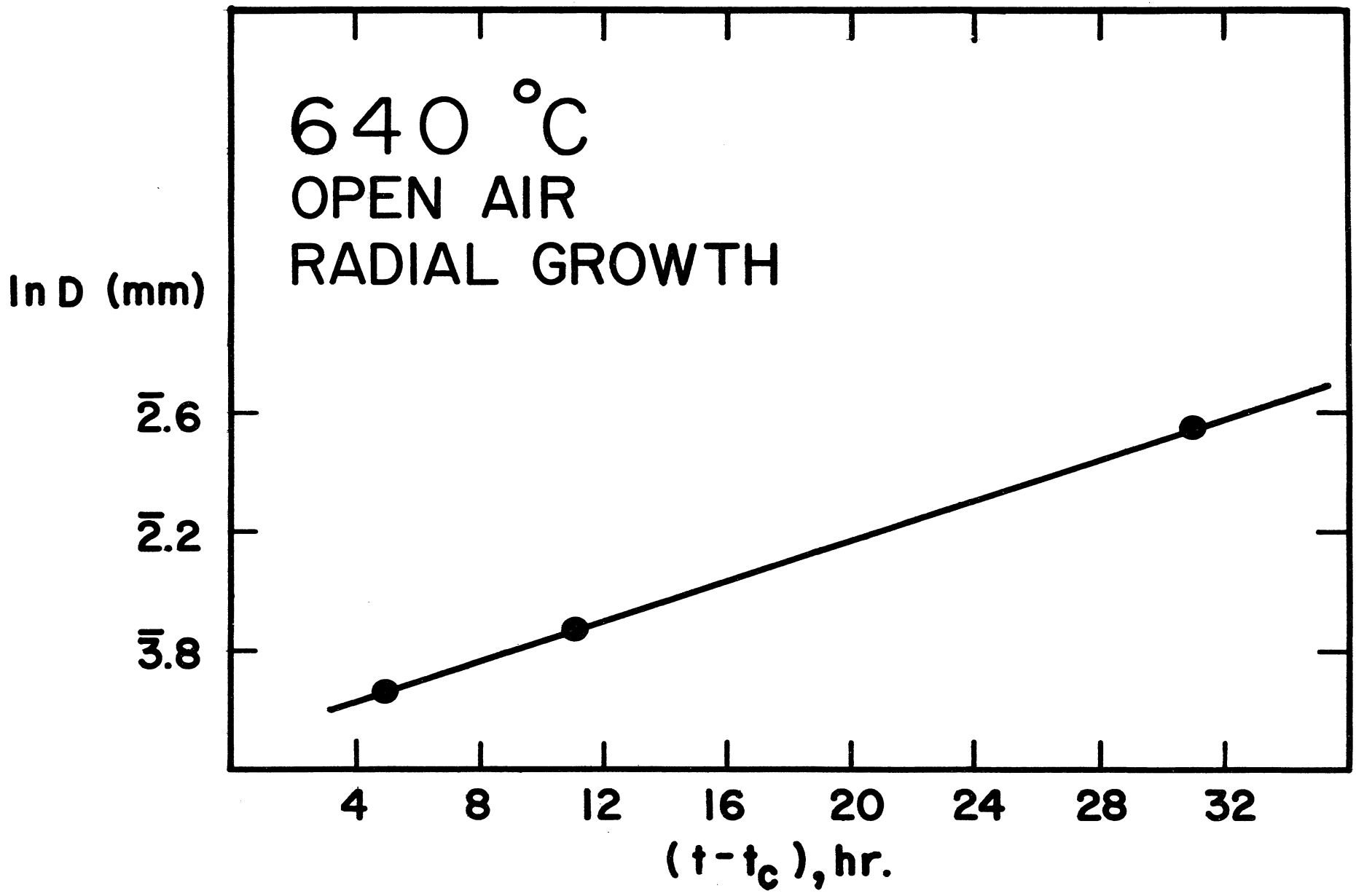

Fig. 10. Radial growth of vanadium pentoxide whiskers plotted according to equation (20).

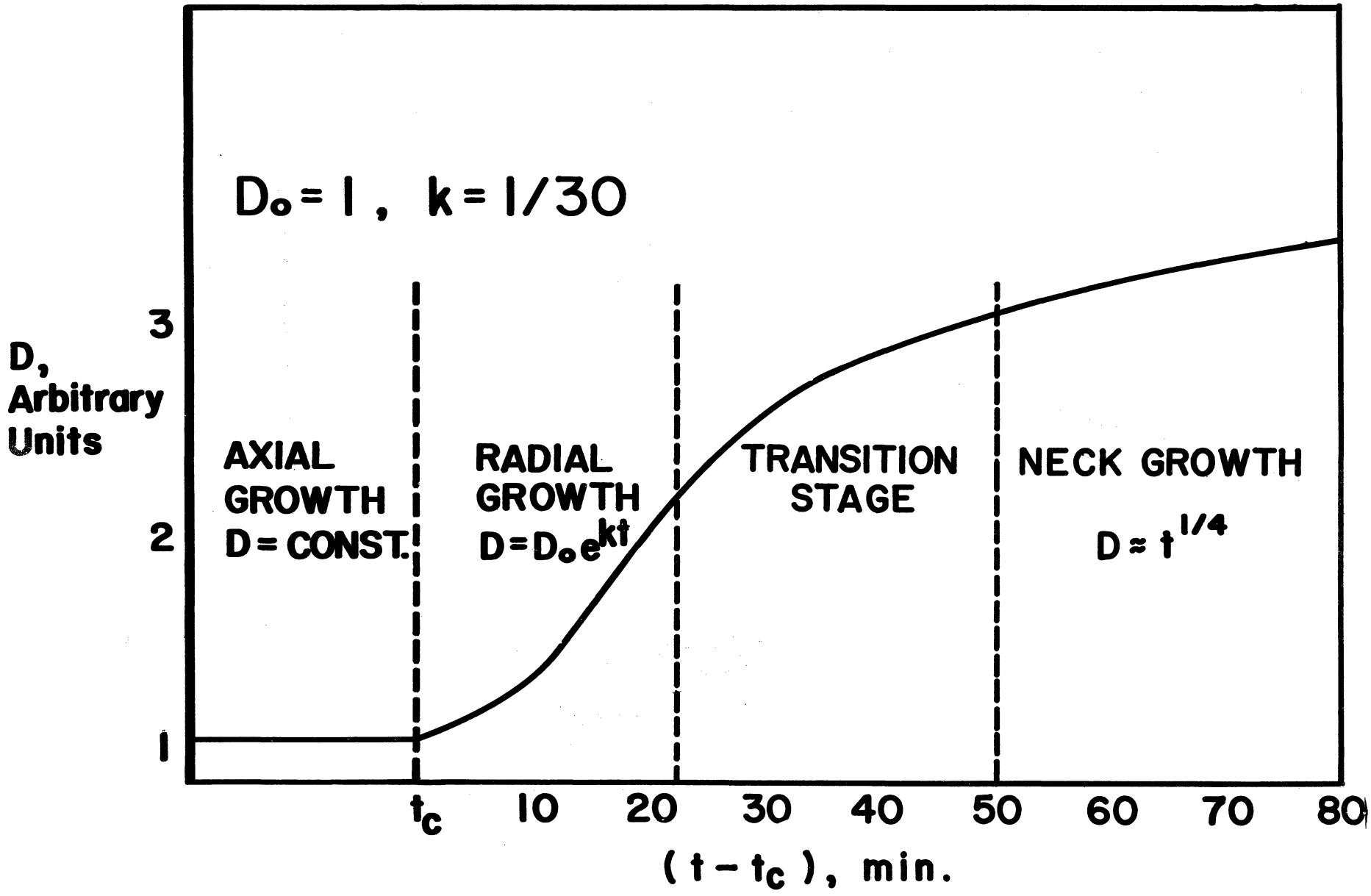

Fig. 11. Initial stages for sintering of vanadium pentoxide microspheres.

DISTRIBUTION LIST

Agency	No. of Copies
Commander, Headquarters AF Office of Scientific Research Washington 25, D.C. Attn: SRQB	5
Commander Wright Air Development Center Wright-Patterson AF Base Ohio Attn: WCRRH Attn: WCRRL Attn: WCRTL Attn: WCRTM-1	4
Commander AF Cambridge Research Center L. G. Hanscom Field Bedford, Massachusetts Attn: Technical Library Attn: CRRF	2
Commander Rome Air Development Center Griffiss Air Force Base Rome, New York Attn: Technical Library	1
Director Office for Advanced Studies AF Office of Scientific Research P. O. Box 2035 Pasadena 2, California	1
Superintendent Diplomatic Pouch Rooms Department of State Washington 25, D.C. For Transmittal to: Commander European Office, ARDC c/o American Embassy Brussels, Belgium	1
Commander Armed Services Technical Information Agency Arlington Hall Station Arlington 12, Virginia Attn: TIPDR	10
Director Research and Development Hq., U. S. Air Force Washington 25, D.C. Attn: AFDRD-RE-3	1
Department of the Navy Office of Naval Research Washington 25, D.C. Attn: Code 423 Attn: Code 421	2
Officer in Charge Office of Naval Research FPO No. 100 New York, New York	1
Commanding Officer Naval Radiological Defense Lab. San Francsico Naval Shipyard San Francisco 24, California	1
Director Research and Development Division General Staff Department of the Army Washington 25, D.C.	1
Division of Research U.S. Atomic Energy Commission Division Office Washington 25, D.C.	1
Oak Ridge National Laboratory P. O. Box P Oak Ridge, Tennessee Attn: Central Files	1

DISTRIBUTION LIST (Concluded)

Agency	No. of Copies
U. S. Atomic Energy Commission Library Branch Technical Information Division ORE, P. O. Box E Oak Ridge, Tennessee	1
Brookhaven National Laboratory Upton, Long Island, New York Attn: Research Library	1
Argonne National Laboratory P. O. Box 299 Lemont, Illinois Attn: Librarian	1
Ames Laboratory Iowa State College P. O. Box 14A, Station A Ames, Iowa	1
Knolls Atomic Power Laboratory P. O. Box 1072 Schenectady, New York Attn: Document Librarian	1
National Bureau of Standards Room 203, Northwest Building Washington 25, D.C. Attn: Library	1
National Science Foundation 1901 Constitution Avenue, N.W. Washington 25, D.C.	1
Director Office of Ordnance Research Box CM, Duke Station Durham, North Carolina	1
Commander Western Development Division P. O. Box 262 Inglewood, California Attn: WDSIT	1
Office of Technical Services Department of Commerce Washington 25, D.C.	1
Document Custodian Los Alamos Scientific Laboratory P. O. Box 1663 Los Alamos, New Mexico	1
Arnold Engineering Development Center P. O. Box 162 Tullahoma, Tennessee Attn: Technical Library	1
Commanding Officer Ordnance Materials Research Office Watertown Arsenal Watertown 72, Massachusetts	1
Commanding Officer Watertown Arsenal Watertown 72, Massachusetts Attn: Technical Reports Section, WAL	1
NACA 1512 H Street, N.W. Washington 25, D.C.	1
Commander Air Technical Intelligence Center Wright-Patterson Air Force Base Ohio Attn: Deputy for Documentation	1
Commander, Headquarters AF Office of Scientific Research Washington 25, D.C. Attn: Technical Library, SREC	2
Commandant AF Institute of Technology Wright-Patterson Air Force Base Ohio Attn: Technical Library, MCLI	1
Commander Wright Air Development Center Wright-Patterson Air Force Base Ohio Attn: Mr. R. Besamson, WCLTY-3	1